Range Focusing in Volumetric SAR: a Phase Recovery Approach

Mehrdad Yaghoobi, Shaun Kelly and Mike E. Davies,
{m.yaghoobi-vaigha , mike.davies}@ed.ac.uk, shaun.i.kelly@gmail.com,
University of Edinburgh, UK

Abstract

Synthetic aperture radar (SAR) systems have been introduced to essentially increase the azimuth resolution. This has been possible by coherently combining the range compressed information along the flying track. The key point is to have a set of calibrated measurements. While the problem of calibration and digitally focusing of the pulses, collected along a single pass, has been significantly investigated, there has been very little attention to the multipass scenario. In this setting the range estimation error can be generally larger and, as a result, conventional range focusing techniques will normally fail to correct such errors. We here investigate the problem of volumetric SAR, where a set of range compressed pulses are provided by multipass circular trials. We demonstrate that the range estimation error causes some structured phase errors, which can be then formulated as a phase recovery problem. We introduce a new range focusing method using Gerchberg-Saxton type phase recovery. We finally show that the new technique is capable of correcting the range error up to a small offset.

1 Introduction

SAR systems are based on this principle that we can generate a synthetic aperture using a moving platform and collect the pulse information from different spacial locations. An accurate knowledge of the location of platform and the scene topography is the necessary part of high resolution SAR imaging. However, neither of these two pieces of information are precisely known for different reasons, including inaccuracy of navigation system and imaging of an unknown area. The conventional approach to calibrate the location information is to use some reference targets with ground truth information about their locations. While such techniques are generally successful, such reference targets rarely exists in the real experiments. As a result, many digital focusing techniques have been proposed, including Phase Gradient Algorithm (PGA), map drift [6] and more recently, sparsity based autofocus [7,9] techniques. In these techniques, we often assume small aperture, far field and/or small errors [6]. As a result, such techniques have some limitations in the wide-angle, large error and possibly digitally chipped SAR imaging [4]. Particularly, any autofocus techniques based on the single phase error per pulse model, *i.e.* the most frequent approach for single pass SAR autofocus, cannot correctly compensate the range error, when it is larger than $\lambda/16$, where λ is the wavenumber [1,6].

Volumetric SAR imaging needs a new set of autofocus techniques, which incorporate the multipass nature of the trials [8], to compensate relatively larger range errors [4]. The most intuitive approach is to extend the prominent point autofocus technique to a three-dimensional setting [3]. This approach needs to have a single dominant bright target in the scene to align the pulses with respect to the range compressed peaks.

We reformulate the effect of range estimation error, in a general setting, and show that such an error appears as a structured phase error in the phase history. We then tackle this problem by formulating it as a phase retrieval problem. Inspired by the Gerchberg-Saxton phase recovery algorithm, we introduce an easy range estimation error correction technique for multipass SAR imaging.

2 Mathematical Model

We formulate the induced error by incorrect estimation of the platform to the scene centre distance, without assuming any limitation for error magnitude. This fact distinguishes our analysis from conventional approaches for small error correction, in which it has been shown a single phase correction per pulse can compensate the image blurring artefact. To facilitate a comparison, we adopted the general notation of [6].
Let $s(t) = \exp(i(\omega_0 t + \frac{\alpha}{2}t^2))$ be the (ideal) continuous-time linear FM chirp waveform, where ω_0, α and t are respectively centre frequency, chirp rate and time. We now assume that $s(t)$ is zero outside the interval $-\tau_c/2 \leq t \leq \tau_c/2$, where $\tau_c = \frac{2\pi B_c}{\alpha}$ and B_c is the chirp bandwidth. If we write the time delay of receiving a transmitted waveform by $\tau_0 + \tau(u)$, where u, τ_0, $\tau(u)$ are respectively distance to the scene centre, round trip delay to the scene centre and u distant from the scene centre in the range direction, the received signal $r_c(t)$ can be presented as follows:

$$r_c(t) = \int_{-u_1}^{u_1} a g(u) \exp(i(\omega_0(t - \tau_0 - \tau(u)) + \frac{\alpha}{2}(t - \tau_0 - \tau(u))^2))du$$

where $g(u)$ is the microwave reflectivity density function,

ISBN 978-3-8007-4228-8 / ISSN 2197-4403

a is a constant related to the propagation attenuation, u_1 is the maximum distance from the scene centre in slant range. If we define $U = \frac{2}{c}(\omega_0 + \alpha(t - \tau_0))$, where c is the speed of wave in free space, and using the fact that $\tau(u)$ is a linear function of u, *i.e.* $\tau(u) = \frac{2u}{c}$, the dechirped signal $\tilde{r}_c(U)$ can be derived as follows:

$$\tilde{r}_c(U) = \int_{-u_1}^{u_1} ag(u) \exp\left(i(\frac{2\alpha}{c^2}u^2 - uU)\right) du \quad (1)$$

Note that we have not used the usual approximation for range compression, which is necessary to be able to use the Fourier slice theorem for inverse imaging, *i.e.* ignoring the quadratic term $\alpha\tau^2(u)$, see for example [6].

2.1 Dechirping with Range Error:

We now investigate the scenario in which we have δR range estimation error. The induced time delay by such an error is $\epsilon = \frac{2}{c}\delta R$. The erroneous dechirped signal $\tilde{r}_c^{\epsilon}(t)$, which has superscript ϵ to emphasised that it is influenced by the error, can be found as follows:

$$\begin{aligned}\tilde{r}_c^{\epsilon}(t) &= \int_{-u_1}^{u_1} ag(u) \exp(i(-\omega_0(\tau(u) + \epsilon) \\ &\quad + \frac{\alpha}{2}((t - \tau_0 - \tau(u))^2 - (t - \tau_0 + \epsilon)^2)))du \\ &= \int_{-u_1}^{u_1} ag(u) \exp(i(-\omega_0(\tau(u) + \epsilon) \\ &\quad + \frac{\alpha}{2}(\tau^2(u) - \epsilon^2) - \alpha(t - \tau_0)(\tau(u) + \epsilon)))du\end{aligned}$$

By substituting the values of $\tau(u)$ and U, we can derive the following equation for $\tilde{r}_c^{\epsilon}(U)$,

$$\tilde{r}_c^{\epsilon}(U) = \exp\left(-i\left(\frac{\epsilon c}{2}U - \frac{\alpha\epsilon^2}{2}\right)\right)\tilde{r}_c(U) \quad (2)$$

In the case $\delta R \ll \rho$, where $\rho = \frac{c}{2B_c}$ is the range resolution, we can simplify (2) and derive,

$$\tilde{r}_c^{\epsilon}(U) \approx \exp\left(i\frac{\alpha\epsilon^2}{2}\right)\tilde{r}_c(U) = \approx \exp(i\beta)\tilde{r}_c(U), \quad (3)$$

which means that the dechirped pulse with range error only has a single phase error per pulse, see for example [6]. In high resolution SAR, δR is in the order of ρ or even larger. In this setting, we need to consider the effect of frequency dependent term, *i.e.* $\frac{\epsilon c}{2}U$. In this setting, it is more convenient to rewrite (2) as follows,

$$\tilde{r}_c^{\epsilon}(t) = \exp\left(-i\left(\alpha\epsilon t + \epsilon(\omega_0 - \alpha\tau_0 - \frac{\alpha\epsilon}{2}\right)\right)\tilde{r}_c(t) \quad (4)$$

This equation clearly shows that the phase error is a function of time.

3 A Phase Recovery Formulation

We have shown that the range estimation error can be formulated as a phase error. We now discretise the signal observation model. Such a discretisation helps us to present the scene and phase history as vectors of finite dimensional vector spaces and the relation, as a linear operator, by a matrix, *i.e.* forward operator. In this setting, we represent (1) in the discrete time domain as follows:

$$\begin{aligned}\tilde{r}_j[m] = \sum_{n=-N/2}^{N/2} ag_j[n] \exp(i(&\frac{2\alpha(\Delta r)^2}{c^2}n^2 \\ &- \frac{2\Delta r}{c}(\omega_0 - \alpha\tau_0)n - \frac{2\alpha\Delta t\Delta r\alpha}{c}nm))\end{aligned}$$

where Δt and Δr are respectively the sampling interval in fast and slow times and g_i is the microwave reflectivity density function of the scene, related to the ith pulse. We can equivalently write this equation in a matrix-vector product form as follows:

$$\tilde{\mathbf{r}}_j = \mathbf{\Phi}\mathbf{g}_j = \mathbf{\Phi}\mathcal{G}\{\mathbf{X}\} = \mathbf{A}_j\mathbf{x} \quad (5)$$

where $\mathbf{X}$ is the discretised reflectivity map of the scene, $\mathbf{x}$ is the vectorised version of $\mathbf{X}$ generated by concatenation of its columns, $\mathcal{G}$ is the integration function along wavefront pattern and $\mathbf{A} = \mathbf{\Phi}\mathcal{G}$ is the linear forward operator. We now put the discretised range compressed pulses $\tilde{\mathbf{r}}_j$'s, from (5), in the columns of a matrix $\tilde{\mathbf{R}}$ and generate a phase history. We note the linear mapping from the scene reflectivity space, *i.e.* $\mathbb{C}^{N\times N}$, to the phase history space by $\mathcal{A}$, *i.e.* $\mathcal{A}\mathbf{X} = \tilde{\mathbf{R}}$. To generate the forward operator, when there exist range estimation errors, we can use (4) and define a matrix $\mathbf{\Gamma} = [\boldsymbol{\gamma}_j]_{j\in\mathcal{J}}$, where $\mathcal{J}$ is the set of index numbers with $|\mathcal{J}| = J$, and the mth element of $\boldsymbol{\gamma}_j$ can be found as follows:

$$\{\boldsymbol{\gamma}_j\}_m = \exp\Big(-i\left((\alpha\epsilon_j\Delta t)m + \epsilon_j(\omega_0 - \alpha\tau_0 - \frac{\alpha\epsilon_j}{2})\right)\Big) \quad (6)$$

where $\epsilon_j = \frac{2}{c}\delta R_j$ is the delay induced by the jth pulse range error δR_j. The forward operator with the delay $\boldsymbol{\epsilon} = [\epsilon_j]$, can be generated by, $\mathbf{\Gamma} \odot \mathcal{A}$, where $\odot$ is an element by element product. In this setting, we can summaries the SAR sensing formulation as follows:

$$\tilde{\mathbf{R}} = \mathbf{\Gamma} \odot \mathcal{A}\mathbf{X}.$$

If we know $\boldsymbol{\epsilon}$, we can use this formula for imaging using standard focusing techniques, *e.g.* polar format algorithm, Back Projection (BP) or sparsity based techniques. In the case of unknown $\boldsymbol{\epsilon}$, this problem is generally called the phase retrieval problem. As we now have some extra unknown parameters, *i.e.* unknown phases of $\mathbf{\Gamma}$, we generally need more samples than before to correct the phase ambiguity. We recall that incorporation of $\mathbf{\Gamma}$ cannot be reformulated as standard pulse by pulse phase correction, for which there are already many successful algorithms. There are some techniques which consider more complicated phase errors and present some techniques for compensating the errors, [9, 10]. However, most of such techniques are based on gradient descent techniques, to reduce the representation errors, and applying some prior model for $\mathbf{X}$, *e.g.* sparsity. Sadly, when the appropriate structure for the phase error matrix $\mathbf{\Gamma}$ has not been considered, we have to use many more pulses to have a well-defined system of equations. This is not feasible in

the practical settings. We therefore need to enforce some structure, *i.e.* similar to that introduced in (6), to make the solution tractable.

In the next section, we present an iterative phase recovery algorithm, inspired by the Gerchberg-Saxton (GS) [5] algorithm, one of the most practical techniques for phase recovery.

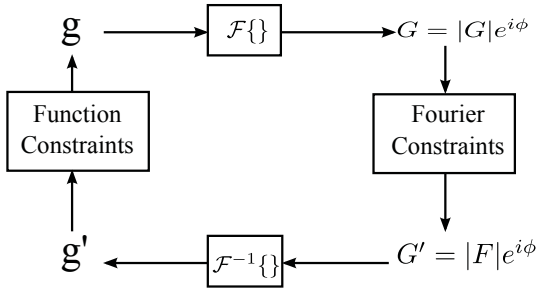

Figure 1: Gerchberg-Saxton (error reduction) algorithm.

4 Focussing by Phase Recovery

When the measurements of a system is linear with some phase ambiguity, which includes the case of completely losing the phase information, we need some phase recovery techniques. Such techniques use the fact that the system has some properties, including linearity, Harmonicity, randomness or an overdetermined nature, and the signal of interest has some properties in spatial/time and/or frequency domain. Such features of the sensing system and the signals have helped researchers of various fields to introduce fundamentally different phase recovery algorithms [5]. While some attention have recently been given to the convex and gradient based techniques, they are not often practical for real size problems [2]. We here introduce a practical iterative phase recovery algorithm for the recovery of $\mathbf{\Gamma}$, which is structurally similar to the standard form of GS algorithm. The schematic of GS algorithm is presented in Figure 1. GS iteratively calculates the Fourier, respectively inverse Fourier, transform and apply signal structures, *i.e.* constraints, in that domain, and alternate the operator, *i.e.* Fourier with inverse Fourier and vice versa, in the other iteration. We can interpret the Fourier and inverse Fourier transforms respectively as forward and backward operators. With some modifications we can instead use other forward/backward operator pairs, to impose the signal constraints in a custom sensing setting. We therefore use SAR forward and backward operators, *i.e.* $\mathcal{A}$ and $\mathcal{A}^H$.

We assume that the SAR imaging system gives us some erroneous phase history $\tilde{\mathbf{R}}_0$, *i.e.* $\tilde{\mathbf{R}}_0 = \mathbf{\Gamma}_0 \odot \mathcal{A}\mathbf{X}_0$, where we do not know the phase error matrix $\mathbf{\Gamma}_0$ and would like to retrieve $\mathbf{X}_0$ from such measurements. We therefore would like to find a pair $(\mathbf{\Gamma}^*, \mathbf{X}^*)$ that minimises the following program,

$$\min_{(\mathbf{\Gamma},\mathbf{X})} \|\tilde{\mathbf{R}}_0 - \mathbf{\Gamma} \odot \mathcal{A}\mathbf{X}\|_F.$$

To simplify the problem and make it suitable for volumetric SAR experiment, we assume that we have a calibrated flight pass and would like to calibrate another flight pass phase history with respect to this data, to be able to coherently use the whole phase history. While other scenarios can be interesting, they need some extra requirements, *e.g.* existence of an isotropic target in the scene. We have another simplification:we assume that the (unknown) induced delay is fixed across the selected aperture, *i.e.* $\forall j, \epsilon_j = \epsilon$. This is a reasonable assumption for short apertures, while it may not be correct for large apertures. A solution is to break the long aperture up to some smaller apertures, when it is possible.

We start the GS framework with $\mathbf{\Gamma} = \mathbf{1}_{N\times J}$, where $\mathbf{1}_{N\times J}$ is the matrix with unit value elements, *i.e.* no phase error and initialise $\mathbf{X}_{ini} = \mathcal{A}^H\tilde{\mathbf{R}}_0$. The signal structure in the phase history domain can be applied by finding the best delay shift ϵ and using the following optimisation program,

$$\epsilon^* = \text{argmin}_\epsilon \|\tilde{\mathbf{R}}_0 - \mathbf{\Gamma}_\epsilon \odot \mathcal{A}\mathbf{X}^{[k]}\|_F, \qquad (7)$$

where $\mathbf{\Gamma}_\epsilon$ is the phase error matrix when $\boldsymbol{\epsilon} = \epsilon\mathbf{1}_J$ and $\mathbf{1}_J$ is a vector of length J with unit value elements. Solving this optimisation program looks difficult, but can be done by exhaustive or line search. As it is a one-dimensional program, it is a computationally tractable task. To induce the sparse (compressibility) structure of the reflectivity map $\mathbf{X}$, we simply soft-threshold the backprojected ϵ^*-delayed phase history $\mathbf{X}^{[k+\frac{1}{2}]} = \mathcal{A}^H(\bar{\mathbf{\Gamma}}_{\epsilon^*} \odot \tilde{\mathbf{R}}_0)$, where "bar" indicates the complex conjugate, as follows:

$$\mathbf{X}_{p,q}^{[k+1]} = \max\left(|\mathbf{X}_{p,q}^{[k+\frac{1}{2}]}| - \frac{\lambda}{2}, 0\right).\text{sign}(\mathbf{X}_{p,q}^{[k+\frac{1}{2}]}), \quad (8)$$

where λ is the threshold parameter and sign operator is the projection onto the unit circle in the complex plane. λ controls the sparsity of the reflectivity map and its larger value makes more small values become zero. This GS type algorithm continues by alternating between reflectivity map and phase-history and using (7) and (8) as induced structures until the new ϵ^* is roughly the same as its value in the previous iteration.

5 Simulation Results

The range estimation error has been observed in most raw data records, see for example [3, 4]. In this paper, we show some controlled synthetic simulations to show the potentials of the proposed range error correction algorithm in comparison with the ground truth information. We chose the general settings of the SAR multipass trial in [3] with a 4° aperture and a four-sparse reflectivity map, to generate the phase history. The location of bright targets was selected at random, and we added some speckle noise to the reflectivity map to make it more realistic. We used the information about passes number one and two, while phase history generated in the pass number one did not have any range error and we induced a 20 cm range error to the pulses recorded in pass number two.

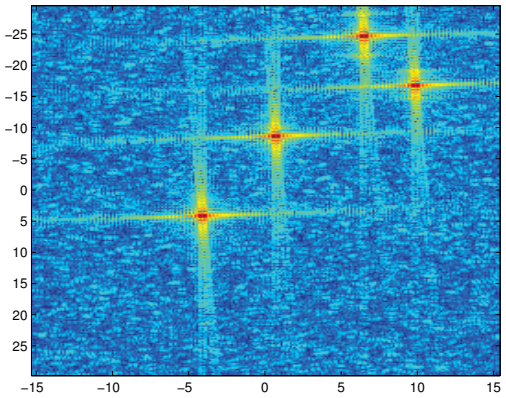

Figure 2: Backprojection of unfocussed phase history.

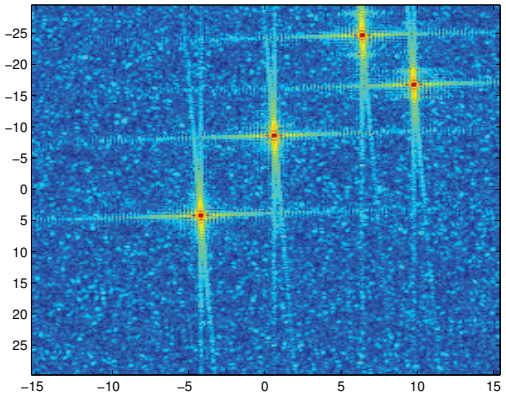

Figure 3: SAR image after range focusing.

Figure 2 shows the backprojection image without any range error correction. A closer look to the image shows that the range error is in the order in which each bright target can be seen in two near, but connected, locations. We applied our algorithm and iterated it 20 times. The final backprojected image with phase correction is shown in Figure 3. It is clear that this image is much sharper and focussed in a comparison with Figure 2. To demonstrate the algorithm capabilities in this experiment, we have plotted the estimated range error, in each iteration, in Figure 4. While we have started from an assumption that is no range error, the algorithm managed to finally recover a parameter of 19 cm, which is close to the ground truth. The ground truth is shown with red dash-dotted plot in this figure.

6 Conclusion

It was explained here why range estimation error is an issue in multipass SAR. We formulated the range error in such data sets and derived some simple formulation for that. The problem was formulated as a structured phase recovery algorithm, while we proposed a derivation of GS algorithm for this purpose. The new algorithm shows a promising result in synthetic data. We have also done some real data simulations and obtained similar results, which have not shown here. More investigations on real data, particularly without reference targets, is left for future work.

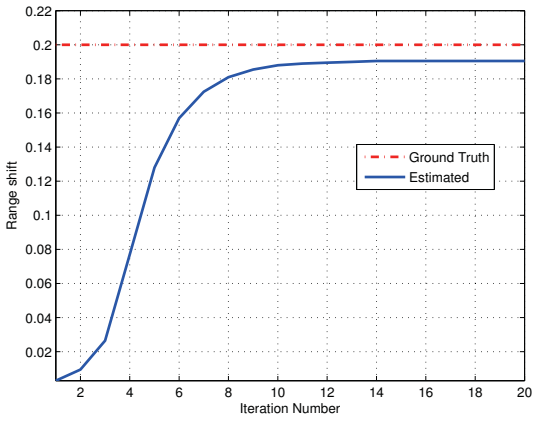

Figure 4: The range error correction factor.

Acknowledgement

This work was supported by EPSRC grants EP/K014277/1 and the MOD University Defence Research Collaboration in Signal Processing.

References

[1] Noah Boss, Emre Ertin, and Randolph Moses. Autofocus for 3d imaging with multipass SAR. In *SPIE Defense, Security, and Sensing*, pages 769909–769909. International Society for Optics and Photonics, 2010.

[2] Emmanuel J Candes, Thomas Strohmer, and Vladislav Voroninski. Phaselift: Exact and stable signal recovery from magnitude measurements via convex programming. *Communications on Pure and Applied Mathematics*, 66(8):1241–1274, 2013.

[3] Curtis H Casteel Jr, LeRoy A Gorham, Michael J Minardi, Steven M Scarborough, Kiranmai D Naidu, and Uttam K Majumder. A challenge problem for 2d/3d imaging of targets from a volumetric data set in an urban environment. In *Defense and Security Symposium*, pages 65680D–65680D. International Society for Optics and Photonics, 2007.

[4] Kerry E Dungan, Joshua N Ash, John W Nehrbass, Jason T Parker, LeRoy A Gorham, and Steven M Scarborough. Wide angle SAR data for target discrimination research. In *SPIE Defense, Security, and Sensing*, pages 83940M–83940M. International Society for Optics and Photonics, 2012.

[5] James R Fienup. Phase retrieval algorithms: a comparison. *Applied optics*, 21(15):2758–2769, 1982.

[6] Charles VJ Jakowatz, Daniel E Wahl, Paul H Eichel, Dennis C Ghiglia, and Paul A Thompson. *Spotlight-Mode Synthetic Aperture Radar: A Signal Processing Approach: A Signal Processing Approach*. Springer Science & Business Media, 2012.

[7] Shaun I. Kelly, Mehrdad Yaghoobi, and Mike Davies. Sparsity-based autofocus for undersampled synthetic aperture radar. *Aerospace and Electronic Systems, IEEE Transactions on*, 50(2):972–986, 2014.

[8] Forest Lee-Elkin. Autofocus for 3d imaging. In *SPIE Defense and Security Symposium*, pages 69700O–69700O. International Society for Optics and Photonics, 2008.

[9] N Ozben Onhon and Mujdat Cetin. A sparsity-driven approach for joint SAR imaging and phase error correction. *Image Processing, IEEE Transactions on*, 21(4):2075–2088, 2012.

[10] Jungang Yang, Xiaotao Huang, John Thompson, Tian Jin, and Zhimin Zhou. Compressed sensing radar imaging with compensation of observation position error. *Geoscience and Remote Sensing, IEEE Transactions on*, 52(8):4608–4620, 2014.